21st International Conference on Composite Materials
Xi'an, 20-25th August 2017

CONCEPTUAL DESIGN OF BRAIDED PREFORMS FOR THE MANUFACTURING OF COMPOSITE LUG

Elena Sitnikova[1], Jun Chen[2*], Jie Yang[2], Bintuan Wang[2] and Shuguang Li[1]

[1] Faculty of Engineering, The University of Nottingham, Nottingham NG7 2RD, UK
[2]AVIC Xi'an Aircraft Design and Research Institute, Yanliang, Xi'an, China
*Presenting author's email: youlingqigai@qq.com

Keywords: Lug, 3D braided composite, Design, Failure modes, Preform

ABSTRACT

This paper aims to explore the feasibility of employing braided composites for manufacturing load-bearing parts of complex geometry. Specifically, design methodology for lugs made of braided composites is proposed. The underlying philosophy is to consider the additional fibre tows suspended in 3D 4-axial braided preform to be the only load bearing components in the composite as a simplified approach. The procedure developed provides a direct estimate of the amount of the additional fibre tows and their intended paths in the braid, so that they can sustain typical types of loading of the lug without failure. A procedure based on netting-type analysis in conjunction with a membrane idealisation has been developed and employed to analyse the tows locally. In this way, the resistance to each of the failure modes can be addressed analytically. The analysis procedure is described in the present paper, and a numerical example based on the procedure has been presented to demonstrate the implemntation of the method, confirming the feasibility of the proposed procedure as a useful means to initiate the design process on a conceptual level.

1 INTRODUCTION

Composite materials rapidly find ever increasing applications in the aerospace engineering, since they deliver similar performance to that of the metallic alloys, yet are substantially lighter. While composite laminates can be employed for manufacturing components of large sizes but relatively simple geometries, for key load bearing parts and components of complex shapes with holes or notches, layered design may no longer be appropriate. As a result, the use of composites for key load carrying parts, e.g. lugs as a part of the joints between wings and fuselage, ailerons and wings, rudder and vertical tail plate, etc. has not been a common practice yet [1]. It is the intention of this paper to explore the feasibility of offering a solution by employing 3D braided composites [2,3]. However, such composites cannot find their practical applications for key load carrying parts and components without delicate design method and appropriate analysis to support such design.

Braiding has the benefits of integrity and versatility in geometry. The former in turn offers superb resistance to impact and fatigue, which are key features one would like to have for key load carrying parts. Versatile braiding architecture allows for the preforms to be fabricated into sophisticated shapes, while maintaining as an integral piece. A typical 4-axial braided fabric preform, see Figure 1(a) as a unit cell, is usually rather compliant and does not provide sufficient properties. By introducing the fibre tows along additional straight axes, e.g. a case as shown in Figure 1(b), desirable improvements can be brought forward. By varying the braiding angle locally and adding or withdrawal of fibre tows appropriately, the cross sections can be adjusted to produce shapes of complicated geometries and also leave cavities, such as holes, without having to cut fibres.

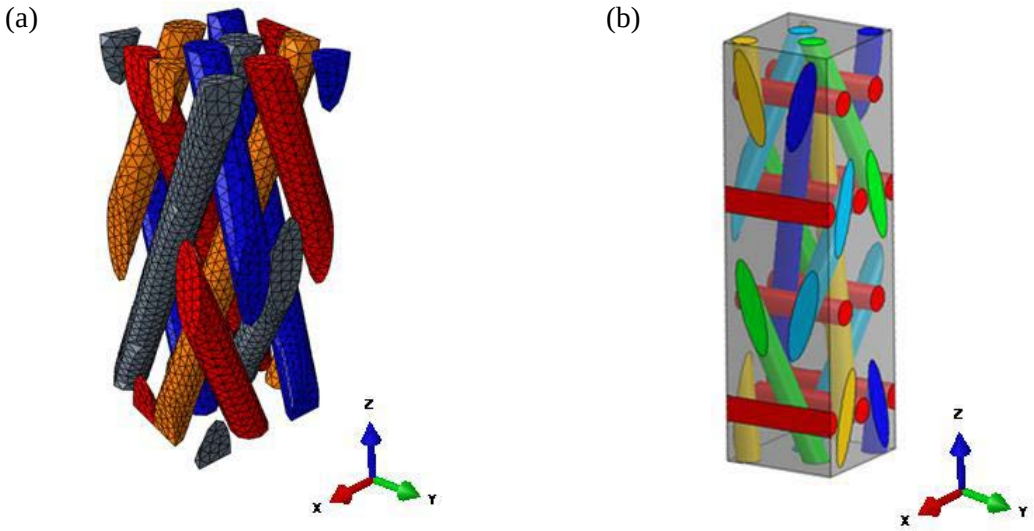

Figure 1: 3D braided reinforcement architectures: (a) conventional 4-axial braid; (b) braid with axial tows.

In present paper, the conceptual aspects of the design of lugs is presented, which is a common part in various structural components, in particular, as a part of the joints. Use will be made of braided preforms in order to deliver such a composite part.

2 CONCEPTUAL DESIGN OF THE FIFTH AXIS TOWS FOR LOAD DISPERSION

To keep the considerations as general as possible, the lug under consideration will have tapered shape (Figure 2), which can reproduce a straight lug easily as a special case.

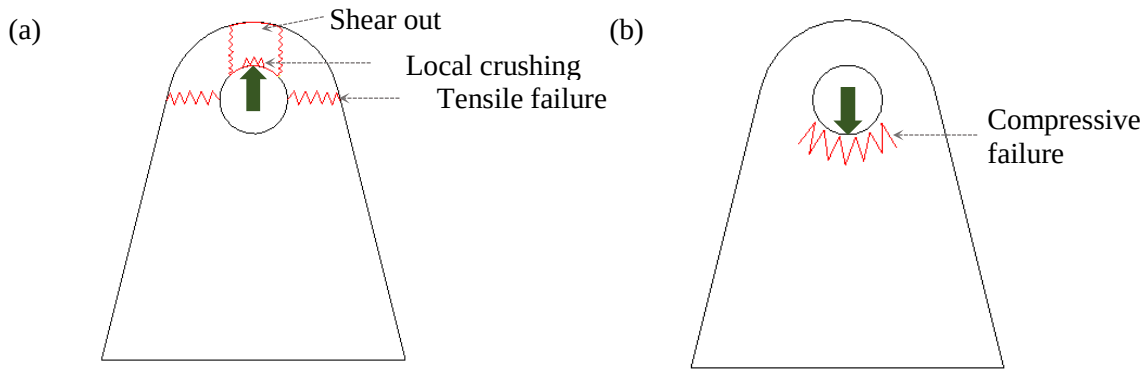

Figure 2: Typical failure modes in the lug loaded in two different modes (a) pulling load; (b) compressive load

The underlying philosophy of the proposed conceptual design is to employ a primarily 4-axial braid as some kind of "matrix" to suspend the axial tows, as schematically shown in Fig. 3, which follow relatively smooth straight or arched paths and could be analysed locally in fashion of "netting analysis". Such axial tows can be embedded in otherwise 4-axial braid during the braiding process. In this way, the resistance to each of the failure modes can be reasonably easily addressed separately.

A lug is usually loaded by the bolt through the hole. Typical loading conditions for a lug are pulling and pushing, as indicated in Figure 2(a) and (b). The typical critical failure modes [4] bear similarities to those of metallic counterparts. Under pulling, loading modes are associated with different areas of the lug. These are (i) tensile failure on the sides, (ii) local crushing at the edge on the top of the hole

against the loading bolt and (iii) shear out of the section in front of the loading bolt, as schematically shown in Figure 2(a), respectively. Under pushing load, compressive failure can be expected around the edge at the bottom of the hole, as schematically shown in Figure 2(b).

However, the failure mechanisms and the order of criticalness of these modes can be rather different. Assuming pulling and pushing loads are of the similar order of magnitude, the most critical mode is likely to be compression failure under pushing loading condition. This is often the least critical aspect for metallic lugs, while under pulling load, tensile failure on one the sides of the hole is usually the most critical mode for metallic lugs.

The main design consideration is that under loading, the majority of the applied load should be sustained without failure by the axial tows. Specifically, those tows will be placed in the braid to form an arched shape. They will be suspended by appropriately interlaced 4-axial braid as the "matrix". Thereby, transverse loading, applied through the hole of the lug, will be converted into the axial tension or compression along the axial tows.

In order to approximately assess load bearing characteristics of thus defined arches, membrane theory [5] based approach was adopted. Arch can be considered a 1D case of membrane shell or a curved string, and the equilibrium relation for it becomes

$$\frac{T}{R} = q\,, \tag{1}$$

where T is the internal longitudinal force, positive for tension and negative for compression, in the arch under the applied distributed load, q, and R is the radius of the curvature of the arch, which is considered to be constant as an approximation over a small range but sufficient for the present interest.

In terms of the material behaviour, the axial tow will be treated as unidirectional (UD) composite, which means that their material properties (strength) in the londitudinal and transverse direction will be the same as those in the UD lamina having the same constituents.

The design exercise as presented here aims to quantify the amount of axial tows required to sustain various types of loading, and to specify the arrangment of those tows of in the braid which would ensure that the part can deliver the desired performance.

2.1 Local crushing and shear out

Relatively, the local crushing mode under pulling load is easy to deal with, and it can be used as the controlling factor for the thickness of the lug. Since in present design exercise the load is assumed to be sustained only by the axial tows, the local crushing under the pulling load is in this case a typical transverse compressive mode.

The pulling load, P_T, applied through the bolt on the hole wall will be distributed uniformly radially in absence of friction between the bolt and the hole wall. Based on the membrane assumption, the internal force, T, in the arch is obtained as

$$T = -\frac{P_T}{2} = qR = \left(\sigma_2 t_T\right) R\,. \tag{2}$$

where σ_2 is the transverse compressive stress in the axial tows, and t_T is the net thickness of the axial tows. The stress resulting from the applied load should not exceed the transverse compressive strength, Y_c, hence

$$\sigma_2 = -\frac{P_T}{2Rt_T} \le -Y_c \tag{3}$$

where Y_c is the transverse compressive strengths of the tows. Re-arranging (3), magnitude of t_T is determined as

$$t_T \geq \frac{P_T}{2RY_c}. \quad (4)$$

The design consideration here is based primarily on the transverse compressive strength of UD composites. This is not the strongest aspect of UD composites as it has not taken advantage of the strength of fibres. Given the fact that there is not viable alternative, it is still a reasonably strong aspect of UD composites. As this particular strength is provided by the matrix which is usually considered as a brittle material. Brittle materials are strong against compression. It has as least used the strongest aspect of the matrix. Relatively, the consistency of the transverse compressive strength is reasonably comparing with some other properties and a designer could have a reasonable level of confidence in this respect.

It should be pointed out that the transverse compression as discussed above is only a means of transmitting the pulling load to fibres, in a way like pulley and rope where the load from the pulley will have be taken by the rope as the tension in the length direction of the rope. The transverse compression corresponds to the direct interaction between the pulley and the rope. The strength of the fibre under such tension will be looked after when the tensile failure mode is considered later.

2.2 Shear failure

The shear out mode is likely to be the least problematic. Shear is usually sustained by matrix. With the 4-axial braid as "matrix", the presence of off-axis fibre tows will offer much stronger resistance to shear than the ordinary matrix. The shear mode of failure will be left for the subsequent strength analysis to check and confirm rather than a major design consideration.

2.3 Tensile failure

The tensile failure on the sides of the hole under pulling load is primaily controlled by the amount of "5th axis fibre tows", which determines the width of the sides once the thickness of the lug is determined from the crushing mode of failure discussed earlier. Sufficient resistance to tensile loading can be ensured relatively easily by taking advantage of high tensile strength of fibres. The axial tows are to be placed within the braid as schematically shown in Figure 3 (a).

Tensile failure is assume to happen across net section as schematically shown in Figure 2. Assuming a uniform tensile stress distribution over the cross section, the magnitude of the critical tensile load, P_T, across the net section can be calculated as

$$P_T = 2A_T X_t \quad (5)$$

where X_t is the longitudinal tensile strength of the tows, and A_T is the area of net cross section given by

$$A_T = bt \quad (6)$$

where b is the lumped width of axial tows on either side of the hole. From Equations (5) and (6), given *t* as determined in(4), it is expressed as

$$b = \frac{P_T}{2X_t t}. \quad (7)$$

With area of net section of the axial tows being defined by (6), and *b* and *t* calculated according to Equations (4) and (7), the lumped area of the fibres in the tows is determined as

$$A_T^f = A_T V_f = btV_f, \quad (8)$$

where V_f is the fibre volume fraction within the tows. Based on (8), number of filaments corresponding can then be evaluated as

$$N_T^f = \frac{A_T^f}{A_{fibre}} = \frac{btV_f}{A_{fibre}} \quad (9)$$

where A_{fibre} is a cross-sectional area of a single fibre. With N_T^f being determined, number of tows of required filament count can be estimated, as will be illustrated later in the example.

With the membrane and frictionless assumption, the tension in the fibres in the axial tows is the same on the sides of the hole and the top of the hole where crushing as another failure mode has been considered earlier. Resistance against tensile stress along the fibre direction is the strongest aspect of fibres and hence that of the UD composites. Relatively, the strength properties in this respect can be obtained most consistently. As a result, as a designer, the level of confidence should be relatively high in this respect as well.

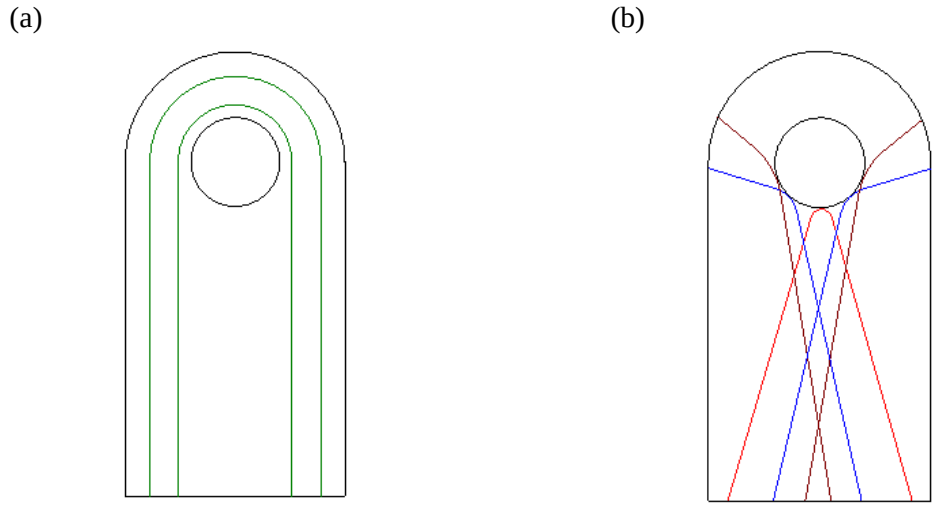

Figure 3: Arrangement of the axial tows as the major loading carrying elements

2.4 Compressive failure under pushing load

The compression under pushing load is the most challenging loading mode. Although it can still be transmitted through transverse compression as in the case of crushing failure mode under the pulling load, such transverse compression is no longer to be sustained be fibre tension anymore. Instead, fibres will have to be subejcted to axial compression to resist the pushing load. Bearing in mind that compression in fibre direction is not a strong aspect for fibres and the associated strength property is rather inconsistent. A designer has to bear these in mind whilst conducting his/her design.

To take advantage of the compressive strength along fibre direction, which is still significant higher that other strengths of the UD composites although not as high as its tensile counterpart, having fibres laid in radial directions around the hole to sustain the interactive force from the bolt in the hole would seem as a natural choice intuitively. However, this should be dismissed first. Carbon fibres are of high stiffness in the fibre direction which will not allow the load to be dispersed to the surrounding material. Premature failure of these fibres would lead to a catastropic consequnce. This is partially responsible for the weaknesses in conventional laminates with bolt holes drilled, having some of the fibres cut. Those in the radial direction could be exposed as the weakness because of their high stiffness, which is excessibated by the influence of free edge effects. This will be avoided in the present design.

Similar to tensile case, axial tows are employed to sustain the applied load. However, under pushing load, their high compressive properties are exploited in an alternative and more compliant manner instead. The axial tows are to be placed as arches, as schematically shown in Figure 3(b). The concept was borrowed from arch bridges in civil engineering [6]. When load is applied through the hole of the lug, the process zone, where failure is likely to happen, is in the vicinity of the hole of the lug, where the stresses are the highest. Therefore, the placement of the axial tows should be such that they can sustain load without failure locally, in the area around the hole of the lug.

In the application for which the present design is intended, the pushing load as illustrated in Figure 2(b) is applied through a bolt. The force given represent the resultant of the actually distributed pressure resulting from the contact between the bolt and hole wall. The idea is to sustain such laod through an array of arches, formed from axial tows, distributed over the lower half of the circumference of the hole as illustrated in Figure 3. The roadmap for the design of those arches is as follows:

1) The concentrated load applied though the hole of the lug is replaced by a statically equivalent load distributed over the lower half of the lug. Unlike for the tensile case, the distribution is non-uniform in general, which is more realistic representation of the actual loading. The non-uniform distribution of the load must be taken into account, since it affects the placement of the load-bearing axial tows near the hole of the lug.
2) The applied distributed load is discretised into the desired number of intevals along the lower half of the circumference of the hole of the lug, each interval corresponding to the specific axial tow arch. For each interval, the magnitude of the resultant force, P_i, and its direction are determined.
3) If the size of the interval is sufficiently small, non-uniformity of the distributed load can be neglected, and it can be represented locally by a uniform distributed load, q_i^* . This distribution can be considered symmetric with respect to the resultant force, which is offset towards the point where the concentrated load is applied at each interval, and is statically equivalent to the resultant force.
4) The uniform distributed load as defined in the previous step is assumed to be transferred on the load-bearing axial tow arch as a distributed load q_i. A simplified scenario is considered, where the radius of curvature of the arches, R_i , is assumed to be constant, the load distribution is uniform and acting only on the curved part of the arch. Distribution q_i should also be statically equivalent to the resultant force.
5) Net area of axial tows sustaining the pushing load is determined,

This procedure is also shown in Figure 4. Application of the procedure to the current design is given below.

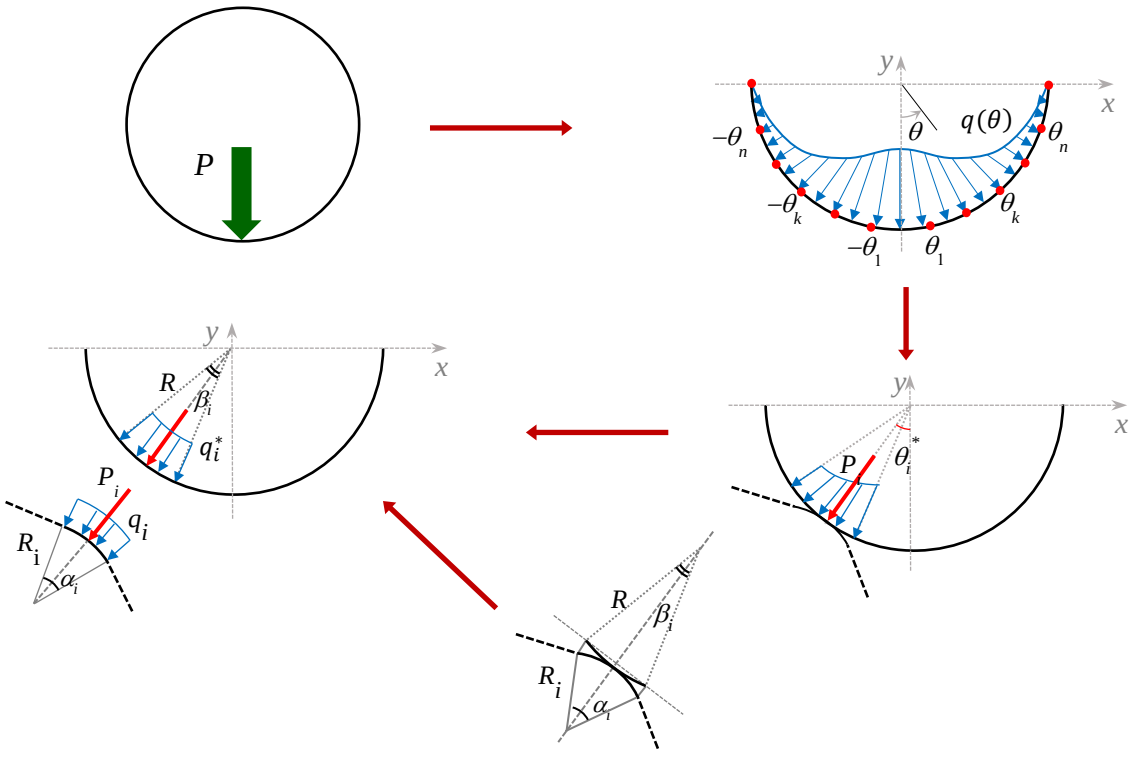

Figure 4: Schematic showing transfer of the load applied around the hole of the lug onto the arches formed by 5th axis fibre tows.

A sinusoidal load distribution, $q(\theta)$, is chosen to represent the applied resultant force, P, as follows

$$q(\theta)=\frac{2P}{R\pi t}\cos\theta,\ \theta\in\left[-\frac{\pi}{2},\frac{\pi}{2}\right], \tag{10}$$

where θ is the angle with respect to the direction of P.

The lower half of the hole is partitioned as follows:

$$\left[-\frac{\pi}{2},-\theta_n\right],\left[-\theta_n,-\theta_{n-1}\right],\ldots,\left[-\theta_1,\theta_1\right],\ldots,\left[\theta_{n-1},\theta_n\right],\ \left[\theta_n,\frac{\pi}{2}\right] \tag{11}$$

For each interval, axial and transverse component of the distribution are calculated. For any interval $\left[\theta_{k-1},\theta_k\right]$, vertical component, $F_{y,i}$, of the resultant concentrated force is calculated as:

$$F_{y,i}=\int_{\theta_{k-1}}^{\theta_k}\cos\theta q(\theta)Rtd\theta=\frac{2P}{\pi}\int_{\theta_{k-1}}^{\theta_k}\cos^2\theta d\theta=\frac{2P}{\pi}\left[\frac{\theta_k-\theta_{k-1}}{2}+\frac{1}{4}\left(\sin 2\theta_k-\sin 2\theta_{k-1}\right)\right] \tag{12}$$

The horizontal component is determined as

$$F_{x,i}=\int_{\theta_{k-1}}^{\theta_k}\sin\theta q(\theta)Rtd\theta=\frac{P}{\pi}\int_{\theta_{k-1}}^{\theta_k}\sin 2\theta d\theta=\frac{P}{2\pi}\left[\cos 2\theta_{k-1}-\cos 2\theta_k\right] \tag{13}$$

Based on (13) and (14), resultant force becomes

$$P_i=\sqrt{F_{x,i}^2+F_{y,i}^2} \tag{14}$$

The angle defining the direction of the force is defined as:

$$\theta_i^*=\arctan\left(\frac{F_{x,i}}{F_{y,i}}\right). \tag{15}$$

This covers steps 1) and 2) of the proposed design procedure. For the next step, static equivalence of the resultant force and uniform distributed load over is established as

$$P_i=\int_{-\beta_i}^{\beta_i}q_i^*\cos\beta Rd\beta=q_i^*R\int_{-\beta_i}^{\beta_i}\cos\beta d\beta=2q_i^*R\sin\beta_i, \tag{16}$$

where β_i are the angles with respect to the resultant force, defined as

$$\beta_i=\left|\theta_i^*-\theta_k\right|. \tag{17}$$

Similarly, static equivalence of the resultant force and the load distributed over the axial tow arch is achieved if the resultant of the distributed load over the arch is equal that obtained from (14) whilst the resultant in the direction perpendicular to P_i vanishes, i.e.

$$P_i=\int_{-\alpha_i}^{\alpha_i}q_i\cos\alpha R_i d\alpha=q_iR_i\int_{-\alpha_i}^{\alpha_i}\cos\alpha d\alpha=2q_iR_i\sin\alpha_i, \tag{18}$$

$$\int_{-\alpha_i}^{\alpha_i}q_i\sin\alpha R_i d\alpha=q_iR_i\int_{-\alpha_i}^{\alpha_i}\sin\alpha d\alpha=q_iR_i\left(\cos\alpha_i-\cos\alpha_i\right)=0, \tag{19}$$

where α_i are the angle with respect to the resultant force, as shown in Figure 4.

Since the two distributions, q_i and q_i^*, are considered to be equal, from Eqs (16) and (18) following equality is established

$$R_i \sin\alpha_i = R\sin\beta_i. \tag{20}$$

This gives the first equation for determining the unknown R_i and α_i. Rearranging Equation (16) yields

$$q_i = \frac{P_i}{2R_i \sin\alpha_i}. \tag{21}$$

Therefore, from (1) and (18), following relation is obtained

$$T_i = q_i R_i = \frac{P_i}{2\sin\alpha_i} \tag{22}$$

from which value of α_i is determined as

$$\alpha_i = \arcsin\left(\frac{P_i}{2T_i}\right), \tag{23}$$

which offers another relation for determining α_i. In order to sustain the applied load without failure, internal force, *T*, should not exceed the critical value:

$$T_i \le T_C{}^i = X_c A_C^i \tag{24}$$

where X_c is the compressive strength of the UD composite, and A_C^i is the lumped area of the cross-section of all the tows forming the arch. Superscript '*i*' indicates that the value of the appropriate parameters vary for different arches.

(a)

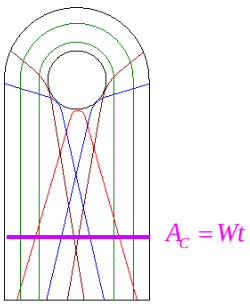

(b)

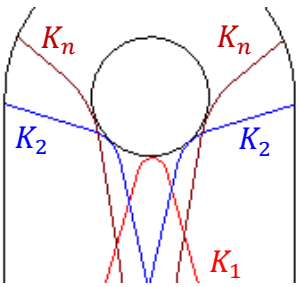

Figure 5 (a) Net area of all axial tows; (b) tows sustaining the pushing load

Parameters A_C^i are unknown, and once they are determined, values of α_i and R_i and can easily be calculated from Eqs. (23) and (20), respectively. To determine values of A_C^i, the net area of all axial tows, A_C, as specified in Figure 5(a), is estimated first. The width of this area is

$$W = 2b + 2R, \tag{25}$$

and the thickness of the area, *t*, should be such that the axial tows can resist crushing under compression locally near the point where the pushing load is applied:

$$q(\theta_i^*) = \frac{2P}{R\pi t}\cos\theta_i^* \le Y_c \quad \Rightarrow \quad t \ge \max_{\theta_i^*} \frac{2P}{Y_c R\pi}\cos\theta_i^*. \tag{26}$$

Next, the total number of the fibres associated with the axial tows sustaining the pushing load is estimated as

$$N_C^f = \frac{A_C^f}{A_{fibre}} = \frac{A_C V_f}{A_{fibre}} - 2N_T^f \,. \tag{27}$$

This can easily be converted to the number of the tows, K_C^f , of the required filament count. The final exercise would be to distribute the tows over the arches sustaining the pushing load, so that

$$K_C^f = K_1 + 2K_2 + \ldots + 2K_n, \tag{28}$$

where K_i is the number of tows in each arch, as shown in Figure 5(b). Then the area of net cross-section for each arch can easily be determined as

$$A_C^i = \frac{N_i A_{fibre}}{V_f}, \tag{29}$$

where N_i is the number of fibres in each arch.

3 DESIGN PROCEDURE AND INPUT DATA

The previous section contains detailed discussions of various considerations of the proposed design procedure, and presents comprehensive derivations of expressions for various parameters of the lug. When applying to practical design, it is not necessary to repeat those derivations every single time. The essential steps of the design procedure are as follows.

1) Lumped thickness and the width of axial tows sustaining the pulling load are evaluated as defined by Equations (4) and (7), respectively;
2) Number of axial tows sustaining the pulling load is estimated based on Equation (9);
3) In order to discretize the load distributed along the hole of the lug into an odd number of intervals symmetrically spread over the lower half of the circumference of the hole, steps defined by Equations (11)-(15) should be carried out;
4) Total number of tows sustaining the pushing load determined following steps defined by Equations (25)-(27).
5) Number of axial tows is assigned to each arch, making sure that the constraint defined by Equation (28) is satisfied. It is reasonable to assume the sinusoidal dependence of the number of tows on the position of the arch along the hole of the lug, so that in the centre, where the magnitude of the applied load is the highest, the number of the tows was the highest, too.
6) Net area of axial tows is determined in each arch according to (29), and with that, half of the central angle α_i, and the radius of curvature, R_i, are calculated for each arch according to Equation (23) and (20), respectively.

Input properties and parameters	Output
• Pulling force, P_T • Pushing force, P • Radius of the hole of the lug, R • Longitudinal tensile strength of the tows, X_t • Longitudinal compressive strength of the tows, X_c • Transverse compressive strength of the tows, Y_c • Fibre volume fraction in a tow • Average area of a single fibre • Filament count in a tow • Number of interval into which the lower half of the hole of the lug is divided	• Lumped width and thickness (t_T and b, respectively) of axial tows sustaining the pulling load • Number of axial tows, required to sustain the pulling load • Net thickness, t, of the axial tows sustaining the pushing load • Number of axial tows, required to sustain the pushing load • Position of the axial tows in the braid near the hole of the lug (radius of curvature R_i and half of the central angle α_i)

Table 1 Input properties and output parameters

The input parameters that need to be specified in order to conduct the design procedure are listed in Table 1 along with the properties which are obtained as the output of the design exercise.

The procedure developed can easily be automated. Specifically, it was incorporated as an Excel spreadsheet, so that the user only needs to modify the input parameters, while the rest of the calculations are done automatically to reflect the changes made.

4 NUMERICAL EXAMPLE OF THE DETERMINATION OF THE 5TH AXIS TOWS

The proposed design methodology is demonstrate by applying it to define the paths of the axial tows in a typical lug. The input parameters, specified in the previous section, are as follows

P_T =20 kN, P = -30kN, R=0.01 m,
X_t =1500 MPa, X_c=450 MPa, Y_c=200 MPa. (30)

The material properties listed in (25) above correspond to T300/BSL914C epoxy UD composite [7]. It is worth noting that the longitudinal compressive strength was discounted by a factor of two, to account for strength losses due to potential distortion of the axial tows in the braid. The fibre volume fraction within the tows was 60%, and the filament count in the tow was taken to be 3000K.

Below the design procedure as outlined in the previous section is followed sequentially.

1) Based on Equation (3), the thickness of the lug is determined as
$$t_T \geq \frac{P_T}{2RY_c} = \frac{20000}{2\times 0.01\times 200\times 10^6} = 5 \text{ mm}.$$
2) Width of the lug on either side of the hole becomes
$$b = \frac{P_T}{2X_t t} = \frac{20000}{2\times 1500\times 10^6\times 0.005} = 1.3 \text{ mm}$$
3) Number of fibres associated with axial tows as defined by Equation (9) is
$$N_T^f = \frac{btV_f}{A_{fibre}} = \frac{0.005\times 0.0013\times 0.6}{4\times 10^{-11}} \approx 104000$$
which corresponds to approximately 35 3K tows.
4) To illustrate the design procedure, the following division of the lower half of the hole is considered:

$$\left[-\frac{\pi}{2},-\frac{3\pi}{8}\right],\ \left[-\frac{3\pi}{8},-\frac{\pi}{8}\right],\ \left[-\frac{\pi}{8},\frac{\pi}{8}\right],\ \left[\frac{\pi}{8},\frac{3\pi}{8}\right],\ \left[\frac{3\pi}{8},\frac{\pi}{2}\right]$$

Consider interval $\left[\frac{3\pi}{8},\frac{\pi}{2}\right]$. Axial component, Y_1, of the resultant concentrated force is calculated according to (13):

$$F_{y,3} = \frac{2P}{\pi}\left[\frac{1}{2}\left(\frac{\pi}{2}-\frac{3\pi}{8}\right)+\frac{1}{4}\left(\sin 2\frac{\pi}{2}-\sin 2\frac{3\pi}{8}\right)\right] \approx -0.01246P \quad (31)$$

The transverse component is determined as given by (14), namely

$$F_{x,3} = \frac{P}{2\pi}\left[\cos 2\frac{3\pi}{8}-\cos 2\frac{\pi}{2}\right] \approx 0.046615P \quad (32)$$

The resultant force (16) becomes

$$P_3 = \sqrt{F_{x,3}{}^2 + F_{y,3}{}^2} \approx 0.048P \quad (33)$$

The angle defining the direction of the resultant force is defined by (16) and its value is

$$\theta_3^* = \arctan\frac{F_{x,3}}{F_{y,3}} \approx 75^\circ \tag{34}$$

The same calculations were repeated for the remaining four ranges of θ.

5) The total number of axial tows sustaining the pushing load was determined to be K_C^f=1056, with their net cross-sectional area being $A_C^f = 0.2\times10^{-3}\,\mathrm{m}^2$.
6) The number of axial tows was estimated, and the values of the half of the central angle and radius of curvature of the arches are calculated.

The results of calculations, outlined above, are summarised in the Table 2.

Range of the angle θ	$\left[-\frac{\pi}{2},-\frac{3\pi}{8}\right]$	$\left[-\frac{3\pi}{8},\frac{\pi}{8}\right]$	$\left[-\frac{\pi}{8},\frac{\pi}{8}\right]$	$\left[\frac{\pi}{8},\frac{3\pi}{8}\right]$	$\left[\frac{3\pi}{8},\frac{\pi}{2}\right]$
Transverse component of the force, $F_{x,i}$, N	-0.0466*P*	-0.23*P*	0	0.23*P*	0.0466*P*
Axial component of the force, $F_{y,i}$, N	-0.0125*P*	-0.25*P*	-0.475*P*	-0.25*P*	-0.0125*P*
Magnitude of the resultant force, P_i, N	0.048*P*	0.34*P*	0.475*P*	0.34*P*	0.048*P*
Angle θ_i^* defining direction of the resultant force	-75°	-42°	0	42°	75°
Number of tows in each arch, K_i	68	196	537*	196	68
Net area of the cross-sections of axial tows for each arch, A_C^i, m^2	13×10^{-6}	38×10^{-6}	51×10^{-6}	38×10^{-6}	13×10^{-6}
Half of the central angle corresponding to the arch, α_i	7.1°	17.3°	18.2°	17.3°	7.1°
Radius of curvature, R_i, m	10.7×10^{-3}	11.2×10^{-3}	12.3×10^{-3}	11.2×10^{-3}	10.7×10^{-3}

*For the middle arch, the number of tows is substantially larger because both legs of the arch contribute to the total net cross-sectional area of axial tows. Therefore, when calculating the net cross-sectional area of this arch, only half of those tows are taken into consideration

Table 2: Calculations of parameters of the arches formed by axial tows corresponding to the different intervals of the hole circumference

In order to assess whether the determined axial tows path would be practical, the steps of design procedure, related to the estimates for the axial tows sustaining the pushing load, were implemented as a Matlab code, and the tow paths were plotted. For the division taken in the example above, the paths of the axial tows are shown in Figure 6(a). As can be seen, axial tows are distributed over the lug in the relatively uniform manner, and the tow paths tend to become straighter for the tows at the sides of the hole of the lug. The latter observation can also be made for when a finer division, with the number of intervals being equal to 13, is considered. The tows paths for this case are shown in Figure 6(b). The build-up of the axial tows can be observed below the hole of the lug. While this design might be more challenging to incorporate in practice, it is reasonable from the mechanical perspective, as the axial tows provide more reinforcement in the area where the applied load magnitude is the highest.

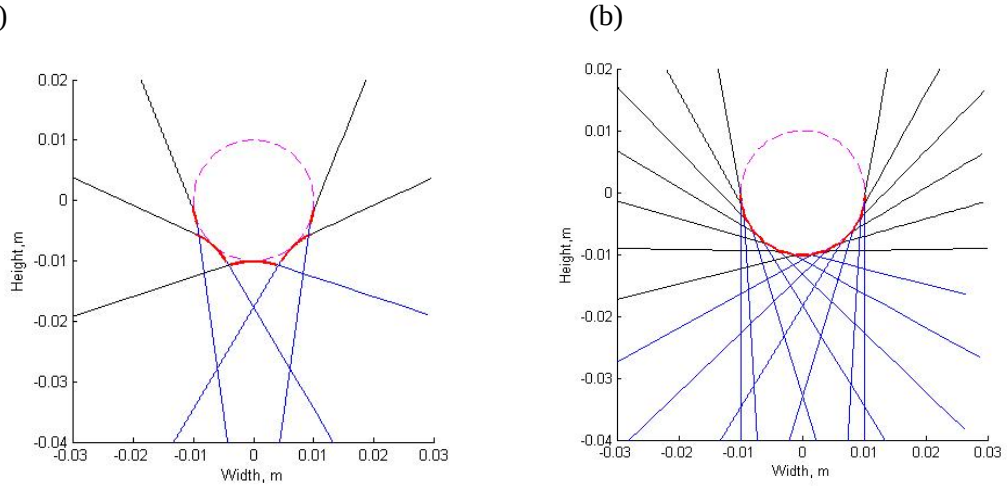

Figure 6 Axial tow paths when the lower part of the hole is discretised into (a) 5 and (b) 13 intervals.

5 CONCLUSIONS

The conceptual design methodology for braided composite lugs has been developed and its detailed description is presented in this paper. Membrane theory based approach was adopted to determine the internal forces in the curved parts of the axial tows. This allowed to estimate the content of the fibre tows sufficient to sustain the loads applied without failure.

The compression under pushing load was identified to be the most challenging loading case. To resist it, use was made of the longitudinal compression strength of the fibres, while the tensile loads were sustained by the longitudinal tensile strength of the fibres. The numerical example presented suggests a feasible conceptual design procedure.

ACKNOWLEDGEMENTS

The financial support for the work carried out from AVIC/FAI under contract number REGS 121681 is gratefully acknowledged.

REFERENCES

[1] CMH-17, Composite Materials Handbooks, Vol. 3 Polymer matrix composites materials usage, design, and analysis, SAE International, Wichita State University, USA, 2012
[2] S. Raha, R. Fangueiro Braided structures and composites: Production, Properties, Mechanics, and Technical Applications, CRC Press, Taylor & Francis Group, Boca Raton, 2016.
[3] Y. Kyosev, Advances in Braiding Technology: Specialized Techniques and Applications, Woodehead Publishing, eBook ISBN: 9780081004265, 2016
[4] M. C. Y. Niu, Composite airframe structures, Hong Kong Conmilit Press limited, 1992.
[5] V.V. Novozhilov, Thin shell theory, Groningen: P. Noordhoff, Netherlands 1964.
[6] Wikipedia, Zhaozhou Bridge (https://en.wikipedia.org/wiki/Anji_Bridge)
[7] P.D. Soden, M. J. Hinton, A. S. Kaddour, Lamina properties, lay-up configurations and loading conditions for a range of fibre-reinforced composite laminates, Composites Science and Technology**,** 58 **(**7**)**, 1011–1022